International Thermal Spray Conference

Vorträge und Posterbeiträge
der gleichnamigen Konferenz

Lectures and Posters
presented at the Conference

Veranstaltet von / Organized by:

DVS – Deutscher Verband für Schweißen und verwandte Verfahren e. V. / DVS – German Welding Society, Düsseldorf

Thermal Spray Society (TSS) of ASM International, Materials Park

IIW/IIS International Institute of Welding, Roissy

Characterization of roughened substrate surface on bond strength of thermal spray deposits

H. Fukanuma, R. Xie, N. Ohno, Toda/J, Y. Fujiwara, Kawasaki/J, and S. Kuroda, Tsukuba/J

Untersuchungen von thermisch gespritzten Schichten unter Berücksichtigung des Einflusses der aufgerauten Substratoberfläche auf die Haftfestigkeit

Inwieweit die Rauheit von gestrahltem Substrat die Haftzugfestigkeit von thermisch gespritzten Schichten beeinflusst, wurde bisher nicht untersucht. Es wurde ebenso noch keine Methode zum Charakterisieren der Substratrauheit oder Topographie in Abhängigkeit zur Haftzugfestigkeit gefunden. Mit einer neuen Methode wird versucht die Oberflächentopographie mit der Haftzugfestigkeit zu vergleichen. Die neuartige Charakterisierung der Rauheit erfolgt mit Hilfe einer dreidimensionalen Oberflächenvermessung mit einem konfokalen Mikroskop. Es wurde ein Experiment entworfen, um die so gemessene Rauheit mit der Haftzugfestigkeit zu vergleichen. Die Untersuchungen haben ergeben, dass ein großer Zusammenhang zwischen der Rauheit von Edelstahl- und Aluminiumsubstraten und der Haftzugfestigkeit der plasmagespritzten Al_2O_3-Schicht besteht.

1 Introduction

It is well known that the adhesive strength of thermally sprayed coatings is greatly influenced by the roughness or topography of the roughened substrate conventionally obtained by grit blasting. It has also been suggested that the adhesive bond strength is caused by such factors as: 1) mechanical anchorage of molten particles into cave-like spaces of the roughened substrate, 2) physical interaction of the van der Vaals force, 3) chemical interaction or metal bonds caused by diffusion of molten particles into the substrate or partial melting of the substrate by hot molten particles [1]. However it has not been made clear how the roughness operates on the adhesion or can be characterized in connection with the strength, and what kind of factors or characteristics of the roughness quantitatively influence the adhesive bond strength.

Studies of how blasting conditions, such as air pressure, blasting materials, particle sizes, and blasting angles, influence the roughness of the substrate have been reported [2-4]. Amada et al studied the relations between the adhesive strength and the substrate surface roughness that was chracterized by fractal dimensions [5,6]. Siegmann et al also reported that fractal dimension or area-scale fractal complexity had good correlation with the adhesive strength [7-9]. Their investigations, however, still lack clear physical interpretations of how the roughness affects the adhesive strength.

As it is important in the thermal spray industry to obtain and control high adhesive bond strength, it is essential to understand how the roughness affects the strength between the coatings and the substrate, and the particle interaction process with the substrate. To clarify the bonding aspect, this study is to propose a new characerizing method of the substrate surface roughness or topography, under the hypothesis that the mechanical friction between the coating and the substrate primarily influences the adhesive strength.

A confocal scanning microscope was used to measure three-dimensional surface profiles, and a computing program was developed for calculation of the numerical data measured with the microscope.

2 Modelling

The modelling is proposed under the assumption that the adhesive strength is caused by the mechanical friction force between the coating and the roughened substrate. The reasons are: 1) Although the factor that has been supposed to be the primary cause of the adhesive strength is anchor effect [1], the idea of the anchor effect is a little vague to deal with numerically, because it is almost impossible to define which is the anchoring point or how much the point contributes to the bonding force. Anchor effect is avoided in the model because of its difficulty to quantify. 2) The micro welding between the splat and the substrate during the deformation and cooling processes has nothing to do with the substrate roughness. Taking the metal bonding effect into account is omitted in the modeling. 3) The van der Vaals force has also no relation to the roughness. It is also neglected in the model.

Suppose that the coating is sprayed on the idealized rough surface on which pyramids are laid down as shown in **Fig. 1**. The side and the height of pyramids are "a" and "$h = n \cdot a$", respectively, where "n" is a constant and $n \geq 0$. The cross section of the deposit cut by the $C-C'$ plane is shown in **Fig. 2-a**. The friction force per unit area along the slope between the deposit and the substrate as shown in **Fig. 2-b** is expressed as

$$f = \mu P \qquad [1]$$

where f, μ, P is friction force, friction coefficient and pressure applied to the interface between the deposit and the substrate, respectively. The friction force applied to a side triangle surface on the pyramid is the product of the friction force per unit area and the triangle's area. Since the perpendicular component of the friction force is described as $f\cos\theta$ and a pyramid has four triangles, when the slope angle is θ as shown in **Fig. 3**, the least force to lift the deposit on a pyramid against the friction force is expressed as:

$$4 \times \text{a side triangle's area} \times f\cos\theta \qquad [2]$$

Since a side triakgle's area $\times \cos\theta$ equals $na^2/2$, Eq. 2 can be written as $2na^2 f$. The force "$2na^2 f$" is the adhesive strength per pyramid. Because the substrate area on which a pyramid is laid is $a \times a$, the adhesive strength per unit area "F" is expressed as:

$$F = \frac{2na^2}{a^2} f = 2nf = 2n\mu P \qquad [3]$$

Equation 3 means that the adhesive strength is proportional to the total of the perpendicular components of the side faces' area on unit area of the substrate.

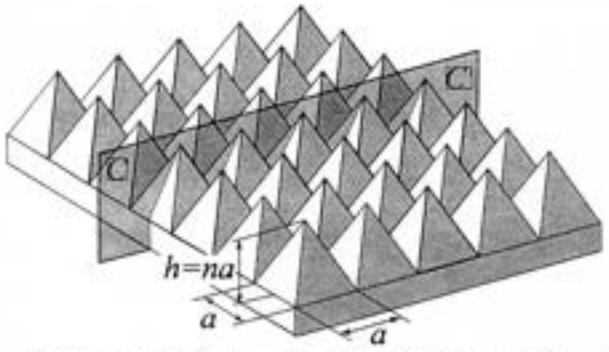

Fig. 1: The idealized rough substrate that pyramids are laid on.

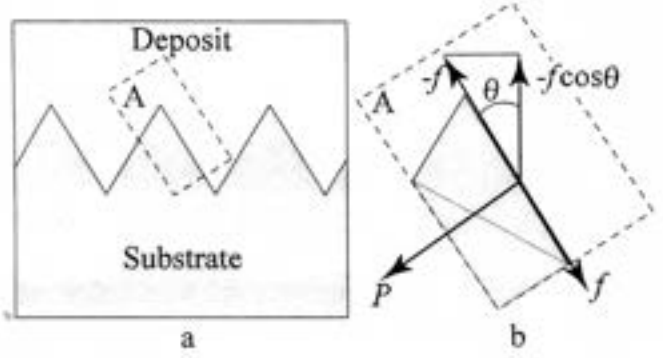

Fig. 2: The friction force between the deposit and the substrate.

To apply this idea to an actual roughened substrate surface, suppose that the rough surface is expressed as $z = f(x, y)$ in orthogonal coordinates (O, x, y, z) as shown in **Fig. 3**, then the infinitesimal friction force df to slide the coating on the infinitesimal area ds of the substrate in parallel to the slope at the point Q is expressed as

$$df = \mu(Q)P(Q)\,ds \qquad [4]$$

where $\mu(Q)$, $P(Q)$ is friction coefficient and pressure at the point Q, respectively. The least infinitesimal force to perpendicularly remove the deposit from the substrate at Q is expressed as

$$df_p = \mu(Q)P(Q)\cos\theta\, ds \qquad [5]$$

where θ is the angle formed by the z axis and a tangential line $\overrightarrow{QU}$ of $f(x, y)$ at Q, and $\overrightarrow{QU}$ is on the plane formed by the normal line $\overrightarrow{QV}$ of ds and the z axis as shown in **Fig. 3**. After integrating Eq. 5 in the region $D(x, y)$ on the curved surface area S given by the function $f(x, y)$, the next equation holds,

$$\int_D df_p = \int_S \mu(Q)P(Q)\cos[\theta(Q)]\,ds \qquad [6]$$

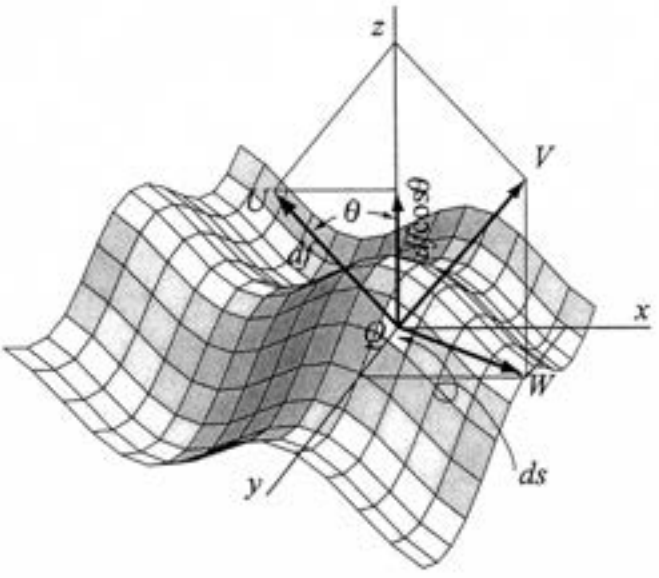

Fig. 3: Schematic illustration of the surface element on the rough surface.

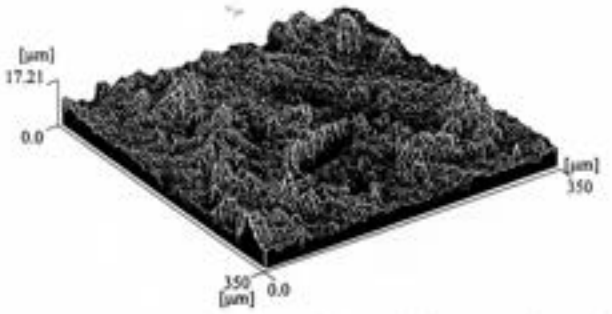

Fig. 4: The surface profile of the stainless steel substrate blasted by Al_2O_3 100 grit in 5 passes.

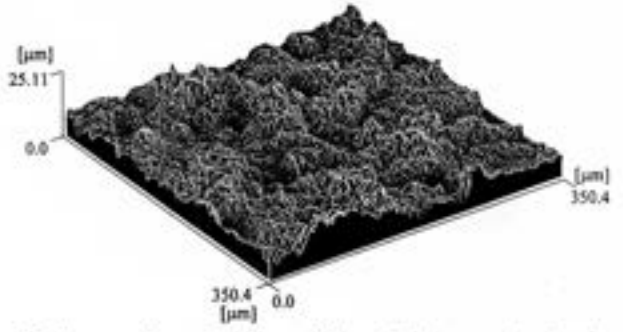

Fig. 5: The surface profile of the stainless steel substrate blasted by Al_2O_3 100 grit in 80 passes.

If $\mu(Q)$ and $P(Q)$ are replaced with $\overline{\mu}$ and $\overline{P}$ which are mean values in the domain D, respectively, the next equation holds.

$$\int_D df = \int_S \overline{\mu}\,\overline{P}\cos[\theta(Q)]\,ds \qquad [7]$$

When the area of the region D is G, the removing force per unit area, namely, the adhesive strength "F" is obtained by dividing Eq. 7 by G as follows;

$$F = \frac{\overline{\mu P}}{G} \int_S \cos[\theta(Q)]ds = \overline{\mu P} R_{bs} = kR_{bs} \qquad [8]$$

where k is a coefficient. The adhesive strength is expressed as a linear equation of the characterised roughness R_{bs}. R_{bs} (Bond Strength Roughness) is the sum of the projection areas of small surface elements on the rough surface on unit area of the substrate.

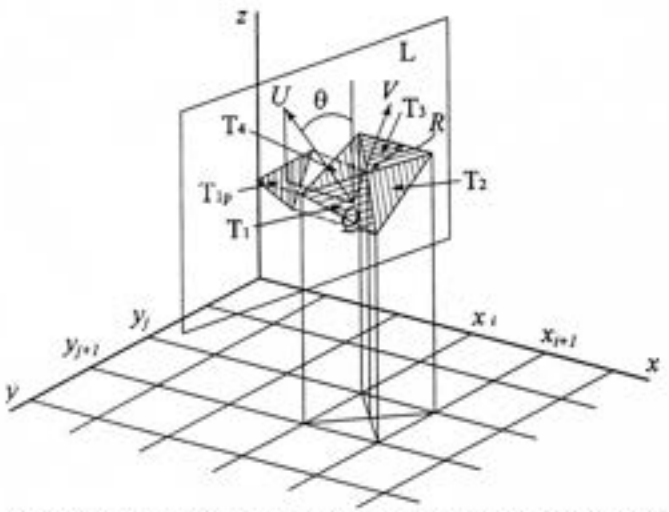

Fig. 6: Schematic illustration of the projection area of part of the rough surface.

3 Measurements of three-dimensional surface profiles

If a three-dimensional profile of the roughened surface can be measured as three-dimensional numerical data, Eq. 8 can easly be computed. A confocal scanning microscope was used to obtain three-dimensional profile data of the blasted substrate [10]. The measuring instrument was the type HD-100D produced by Lasertec Corporation. Typical surface profile examples of blasted substrates measured by the HD-100D with a 50 power objective lens are shown in **Fig. 4** and **5**. The data measured with the confocal microscope are obtained as a set of numerical values given by the formula $z_{ij} = f(x_i, y_j)$. To calculate Eq. 8 from the numerical data, as shown in **Fig. 6**, the point R was determined by taking the average of z_{ij}, $z_{i,j+1}$, $z_{i+1,j}$ and $z_{i+1,j+1}$ as z position value, $(x_i + x_{i+1})/2$ as x position value and $(y_j + y_{j+1})/2$ as y position value. The four triangles, T_1, T_2, T_3 and T_4, can be constructed as shown in **Fig. 6**. The area s_1 of the triangle T_1 can be determined, as the three vertices of T_1 are known. The angle θ between the z axis and the tangential line QU can be determined, because QU is on the intersection of the plane formed by the z axis and the normal line $\overline{QV}$ of the triangle T_1 and the T_1 plane. Then, $\cos\theta \cdot s_1$ which equals T_{1P}, the projection area of the triangle T_1 toward plane L, is determined. The projection areas of the other triangles are determined in the same manner. Equation 8 can be calculated by the sum of $\cos\theta \cdot s$ in the measured region.

4 Experimental procedures

The two kinds of substrate metal used for the experiment were aluminum and stainless steel. The dimensions of the cylindrical specimens were 20 mm diameter and 45 mm long. Conventional suction type blasting equipment was used with a grit feeding device newly developed to ensure the accurate feed rate, and a six-axis robotic device was mounted in the equipment to control the traverse speed, pitch, stand-off distance and angle of the blasting nozzle. The blasting material was Al_2O_3 100 grit and the blasting nozzle diameter was 9 mm. The specimens were blasted under the conditions that the traverse speed, traverse pitch, stand-off distance and angle were 1000 mm/sec, 10 mm, 120 mm and 90 deg., respectively. The other conditions are shown in **Table 1**. After eleven test pieces were blasted under each set of blasting conditions, one specimen was used to measure the three-dimensional surface profile and the other ten were plasma sprayed for the bonding tests. The measured area of the microscope was 350.4 μm x 350.4 μm and the resolution was 1/900 of each side of the view area. Five places on each test piece were measured and the average was used as the R_{bs} value because the measuring area was too small to use a single point value as the representative of the specimen.

Table 1. Blasting conditions

No. of TP	No. of passes	Feed rate [g/min]
#1	1	700
#2	2	700
#3	5	700
#4	10	700
#5	20	700
#6	40	700
#7	80	700
#8	2	455
#9	5	455
#10	11	455

Table 2. Plasma spray conditions

Arc current		850 A
Arc Voltage		38 V
Arc gas	Ar	50 PSI
Secondary gas	He	100 PSI
Spray distance		100 mm
Powder feed rate		20 g/min

The plasma torch used to spray the specimens was the type SG-100 of Praxair Surface Technologies, Inc. White alumina (particle sizes 10 – 44 μm) was used as the spray material to avoid the possibility of metallic bonding, all the test pieces were plasma sprayed at the same time and the coating thickness was approximately 480 μm. The spray conditions are shown in **Table 2**. Tensile adhesive strength measurements were performed in accordance with Japanese industrial standard H8664.

5 Results and discussion

The relations between the tensile adhesive strength and the number of blasting passes on stainless steel and Al substrates are shown in **Fig. 7** and **8**, respectively. These graphs show that the strength on stainless steel increases as the number of blasting passes until 40 passes, on the other hand, the strength rise on Al stops at 10 passes. These results show that grit blasting has a limitation for obtaining further topographical complexity to contribute to the bond strength in thermal spray coatings. To obtain greater strength, another preparation process may need to be developed. From the graphs, it also appears that soft metals such as Al are roughened faster than hard metals. **Fig. 9** and **10** show the relations between the characterized roughness R_{bs} and the number of the blasting passes.

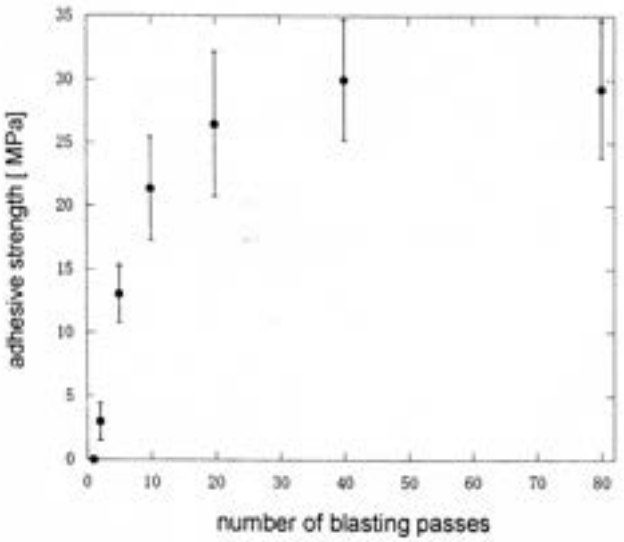

Fig. 7: The relationship between the adhesive strength of WA and the number of blasting passes on stainless steel.

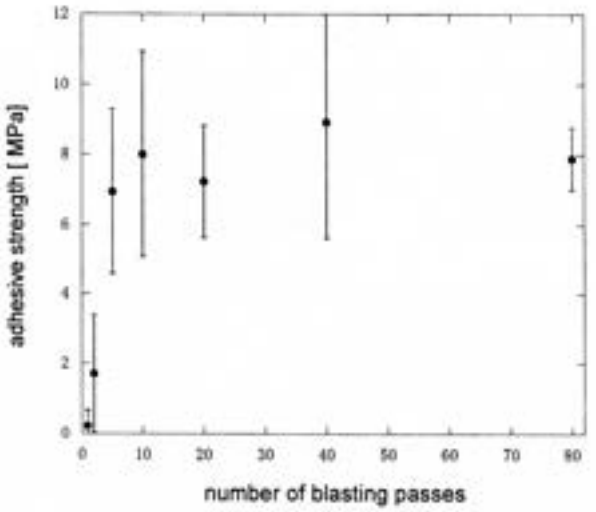

Fig. 8: The relationship between the adhesive strength of WA and the number of blasting passes on Al.

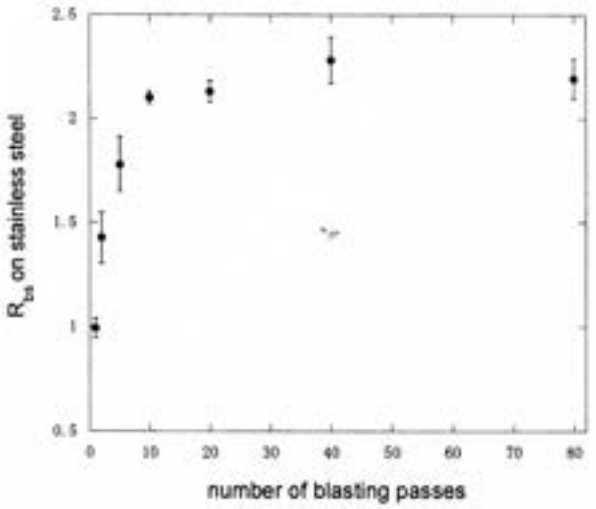

Fig. 9: The relationship between R_{bs} and the number of blasting passes on stainless steel

The curves in **Fig. 7** and **9** show a similarity, and **Fig. 8** and **10** also show the same trend. The relations between the adhesive strength and R_{bs} on stainless steel and Al are shown in **Fig. 11** and **12**, respectively. These graphs show the strong correlations between the adhesive strength and Bond Strength Roughness R_{bs}. R_{bs} shows much better correlations compared with the relations between the strength and Ra roughness shown in **Fig. 13** and **14**. In particular, the correlation between the strength and roughness Ra shows greater deviation in the higher bonding region. Both correlation curves shown in **Fig. 11** and **12** are slightly quadratic, whereas the model shows linear relations with the strength and R_{bs}. This may imply the measurements with confocal microscope lack accuracy in describing the real topography of the rough surface or there are other factors, excepting friction force, to be considered in linking with the strength

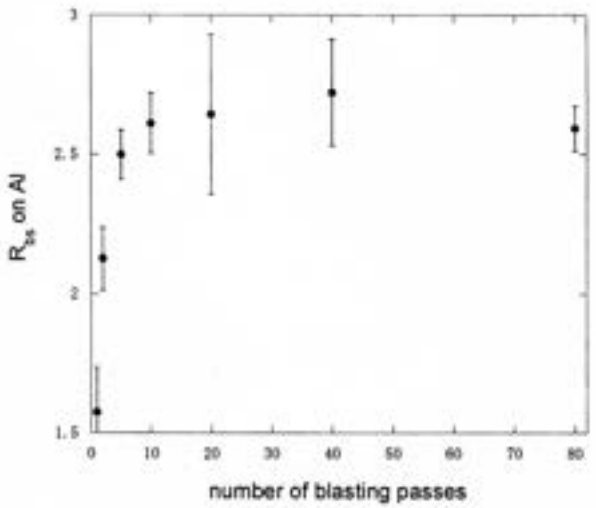

Fig. 10: The relationship between R_{bs} and the number of blasting passes on Al

The maximum strengths on Al and stainless steel are nearly 9.0 and 30 MPa, respectively, as shown in **Fig. 11** and **12**. The maximum strength on Al is nearly one third less than that on stainless steel, though R_{bs} on Al is larger than that on stainless steel. Since the strength is shown as the formula $F = \overline{\mu P} R_{bs}$, the differences of the bond strength between stainless steel and Al come from the difference from the friction coefficient or the pressure applied to the substrates. The pressure on Al might be larger than that of stainless steel, because the thermal expansion coefficient of Al is larger than that of stainless steel. It appears that the friction coefficient on Al is smaller than that on stainless steel, or that the deposit on Al easily separates from the substrate because Al metal readily deforms during tensile test. Provided that the fiction coefficient between the deposit and Al is small, the splat contact area on Al may be smaller than that of stainless steel because the higher thermal conductivity causes the splat not to wet the Al substrate as thoroughly during the flattening and cooling processes.

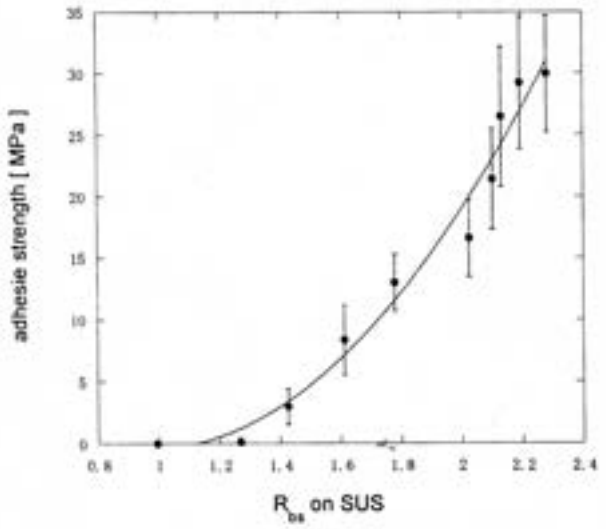

Fig. 11: The relationship between the adhesive strength and R_{bs} on stainless steel.

The fact that the adhesive strength of the deposits on the one pass blasted substrates was zero MPa for stainless steel and smaller than one MPa for Al, as shown in **Fig. 7** and **8**, respectively, shows that the van der Vaals and chemical interaction forces do not contribute to the strength in the extent of this experiment, because the zero or nearly zero strength of the deposits on the slightly roughened substrates means that these forces which must fundamentally cause the adhesive strength of the deposit even on a flat and smooth substrate are nil or negligibly small. The sharp rise of the bond strength with the number of passes or the roughness R_{bs}, as shown in **Fig. 7**, **8**, **10** and **11**, also intensifies that only substrate roughness causes adhesive strength.

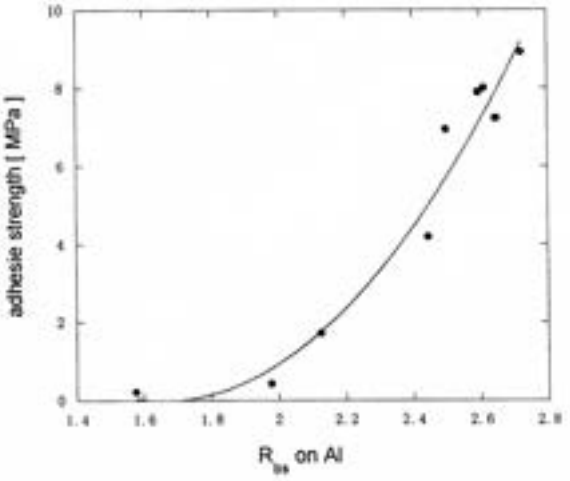

Fig. 12: The relationship between the adhesive strength and R_{bs} on Al.

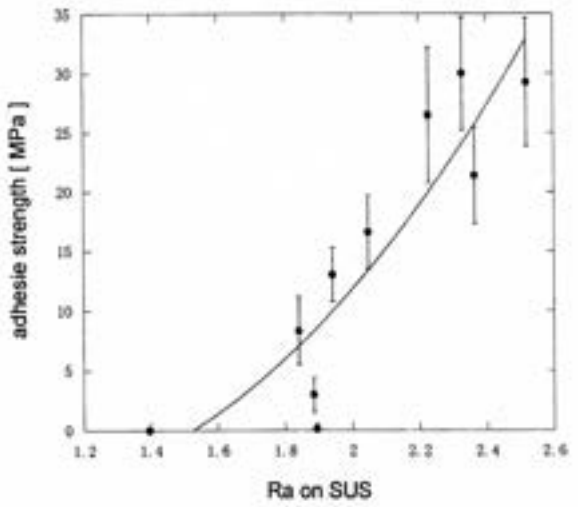

Fig. 13: The relationship between the adhesive strength and Ra on stainless steel.

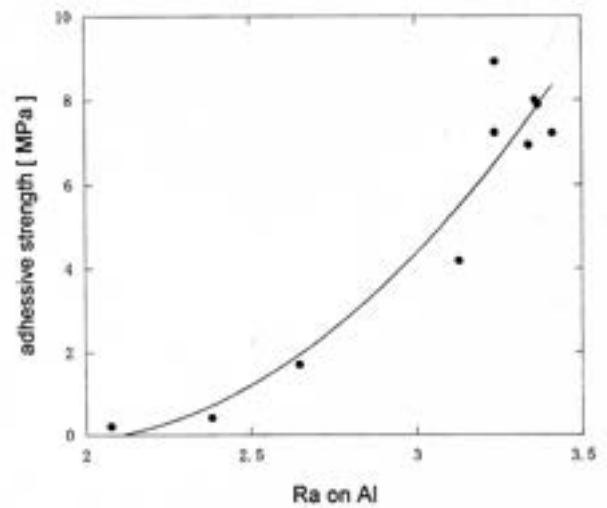

Fig. 14: The relationship between the adhesive strength and Ra on Al.

6 Conclusions

A new method characterizing blasted substrate surface was developed under the assumption that the bonding strength is caused by friction force between thermal sprayed deposit and the substrate. Bond Strength Roughness R_{bs} was introduced from the model and it was shown that R_{bs} had a strong correlation with the adhesive strength.
Although R_{bs} on Al substrate was larger than that on stainless steel under the same blasting conditions, the adhesive strength on stainless steel was much stronger than that on Al.

7 Acknowledgements

Mr. T. Ode at Lasertech Corporation provided important advice on the principle of confocal microscopy and the measurement method, and Mr. O. Takase and Mr. M. Suwa assisted us in performing the three-dimensional measurement of the blasted specimens.

8 Literature

[1] Matejka D. and Benko B.: Plasma Spraying of Metallic and Ceramic Materials. Published by John Wiley and Sons Ltd. 1989, pp. 91/95.

[2] Wigren J.: Grit-Blasting As Surface Preparation Before Plasma Spraying. Advances in Coatings Technology, 1987 NTSC, pp. 99/104.

[3] Mellali M., Grimaud A. and Fauchais P.: Parameters Controlling the Blasting of Substrates for Plasma Spray. Thermal Spray Industrial Applications, 1994, pp. 227/232.

[4] Yankee S. J., Pletka B. J. and Salsbury R. L.: Quality Control of Hydroxylapatite Coatings: The Surface Preparation Stage: Properties, Processes and Applications, 1991, pp.475/479

[5] Amada S., Yamada H., Yematsu S. and Saotome Y.: Modeling and Measurement of Adhesive Strength of Thermal Sprayed Coatings, Thermal Spray: International Advances in Coatings Technology, 1992, 915/920.

[6] Amada S., Hirose T. and Tomoyasu K.: Introduction of Fractal Dimension to Evaluation of Adhesive Strength, Thermal Spraying: Current Status and Future Trends, 1995, pp. 885/890.

[7] Siegmann S. D. and Brown C. A.: Scale-Sensitive Fractal Analysis for Understanding the Influence of Substrate Roughness in Thermal Spraying, Thermal Spray: A United Forum for Scientific and Technological Advances, 1997, pp. 665/670.

[8] Siegmann S. D. and Brown C. A.: Investigation of Substrate Roughness in Thermal Spraying by A Scale-Sensitive 3-D Fractal Analysis Method, Thermal Spray: Meeting the Challenges of the 21st Century, 1998, pp. 931/836.

[9] Siegmann S. D. and Brown C. A.: Surface texture correlations with tensile adhesive strength of thermal sprayed coatings using area-scale fractal analysis, 1999 United Thermal Spray Conference Proceedings, pp. 355/360.

[10] Confocal Microscopy edited by T. Wilson, 1990 Published by Academic Press Limited, pp. 7/30.